Sulfated lactose-modified chitosan. A novel synthetic glycosaminoglycan-like polysaccharide inducing chondrocyte aggregation

Chiara Pizzolitto [a], Fabiana Esposito [b], Pasquale Sacco [c], Eleonora Marsich [a], Valentina Gargiulo [d], Emiliano Bedini [b], Ivan Donati [c,*]

[a] Department of Medical, Surgical, and Health Sciences, University of Trieste, piazza dell'Ospitale 1, I-34127 Trieste, Italy
[b] Department of Chemical Sciences, University of Naples Federico II, Complesso Universitario Monte S. Angelo, via Cintia 4, 80126 Napoli, Italy
[c] Department of Life Sciences, University of Trieste, via Licio Giorgieri 5, 34127 Trieste, Italy
[d] Istituto di Scienze e Tecnologie per l'Energia e la Mobilità Sostenibili, STEMS-CNR, Napoli, Italy

ARTICLE INFO

Keywords:
Lactose-modified chitosan
Sulfation
hMSC-BM
Cell aggregation

ABSTRACT

Lactose-modified chitosan (CTL) is sulfated using SO_3·py or SO_3·DMF as sulfating agents. The two products are characterized by elemental analysis, FT-IR, ^1H,^{13}C-DEPT-HSQC and ^1H,^{13}C-HSQC-TOCSY experiments which allow the extent and selectivity of chemical sulfation to be determined. Dynamic Light Scattering shows a pH-dependent association of the sulfated polysaccharides which are described as flexible by the Smidsrød's B parameter and the intrinsic viscosity at infinite ionic strength. Shear viscosity and intrinsic viscosity show that sulfation protocols lead to chain scission which is more pronounced when SO_3·DMF is used. The sulfated samples are able to induce aggregation of human bone marrow mesenchymal stem cells, resulting in the formation of smaller nodules compared to the unmodified CTL sample. Over time, the sample with the higher degree of sulfation allows further aggregation between cell clusters while the sample with the lower degree of sulfation shows dissolution of the aggregates.

1. Introduction

Lactose-modified chitosan, commonly referred to as Chitlac and commercially available as CTL, is a novel polysaccharide that overcomes the limitations of chitosan in terms of solubility at neutral pH and the possibility of synergistic solutions with polyanions (Donati et al., 2005; Donati et al., 2007; Pizzolitto et al., 2020). CTL is obtained by a *N*-alkylation reaction from chitosan, a polysaccharide consisting of β-1→4 linked D-glucosamine units interspersed with residual *N*-acetyl-D-glucosamines (Sacco et al., 2020). In addition to the physicochemical aspects, CTL shows interesting properties for tissue engineering applications for cartilage, bone, and nerve tissue (Marsich et al., 2008; Medelin et al., 2018; Travan et al., 2012). In combination with hyaluronic acid, CTL neutralizes the upregulation of IL-1β, TNF-α and Gal-1 and the gene expression of metalloproteinases (MMPs) (Tarricone et al., 2020). In addition, several authors have reported the ability of lactose-modified chitosan to induce three-dimensional (3D) cell aggregates in chondrocytes (Donati et al., 2005; Marcon et al., 2005; Tan et al., 2010) and adipose-derived stem cells where the formation of spheroids is described as prerequisite for commitment to the chondrogenic lineage in vitro (Tan et al., 2013). Recent studies show that aggregation of mesenchymal stem cells increases the potential for differentiation to other lineages (Sart et al., 2014). In fact, 3D spheroidal cell aggregates are commonly considered more physiological than cells adhering on surfaces (bidimensional or 2D cultures) (Cesarz & Tamama, 2016). Given the differences in mechanical properties between ordinary 2D cultures on plastic surfaces and 3D cultures, it is likely that spheroids exhibit a difference in mechanophysical properties (Sart et al., 2014). To this end, there is increasing work on the development of synthetic supports for 3D cultures and organoids assembly (Aisenbrey & Murphy, 2020).

Sulfated glycosaminoglycans (GAGs) play a central role in processes such as angiogenesis, cancer response and various other biological events (Bedini et al., 2019). GAGs, the major component of the cartilage–specific extracellular matrix, regulate the expression of the chondrocyte phenotype and support chondrogenesis. Chondroitin sulfate has been proposed for the therapy of articular cartilage osteoarthritis (Bishnoi et al., 2016) and it is used as a slow-acting drug for

* Corresponding author.
E-mail address: idonati@units.it (I. Donati).

Accepted 17 March 2022

symptomatic osteoarthritis (Reginster et al., 2017; Schneider et al., 2012). The negatively charged chondroitin sulfate binds to proteins in the extracellular matrix and thus contributes to regulate cellular activities (Silbert & Sugumaran, 2002). It has been suggested that the ability of sulfated GAGs to bind proteins such as growth factors and chemokines (Shute, 2012), depends on the sulfation pattern, although a complete and comprehensive understanding of this aspect is still pending. However, it is known that the presence of negative charges is a key aspect for the vast majority of such interactions (Berven et al., 2013). All these considerations explain the great attention paid to the use of sulfated GAGs in the development of biomaterials, either as such or in combination with other polysaccharides. Recently, the biological activity of CTL was studied after additionally grafting sulfated polysaccharides such as heparin. It was shown to enhance attachment, proliferation, viability, and GAG secretion of chondrocytes within 3D aggregates (Tan et al., 2008).

The major drawback in the use of sulfated GAGs is the variability of their chemical structure depending not only on the animal source but also on the physiopathological conditions of the individual head of cattle, as well as the possible presence of impurities such as oversulfated species that could lead to adverse effects (Guerrini et al., 2008). Therefore, there is a constant search for semisynthetic GAGs mimics obtained by regioselective sulfation of widely available polysaccharides. A chemical sulfation approach based on multistep regioselective protection(s)-sulfation-deprotection sequence has been successfully applied to several polysaccharides (Bedini et al., 2017). With this approach, different sulfation patterns can be achieved, depending on the efficient application of the protecting group installation and cleavage developed for synthetic carbohydrate chemistry to polysaccharides. This approach has recently been used for the regioselective sulfation of microbial-sourced polysaccharides such as curdlan (Vessella et al., 2021) and unsulfated chondroitin (Vessella et al., 2019).

An alternative approach involves the direct chemical sulfation, which occurs in a single step and avoids the use of protecting groups. While the regioselectivity of these approaches is generally a problem, the presence of highly reactive functional moieties such as primary hydroxyl or amino groups along the polysaccharide chain overcomes this limitation to some extent. In this sense, sulfated alginates with defined structures were prepared and showed functions equivalent to those of heparin (Doncel-Pérez et al., 2018; Revuelta et al., 2020).

The present manuscript deals with the chemical modification of CTL by introducing sulfate groups. Since this is the first work dealing with the obtainment of sulfated CTL derivatives, a direct chemical sulfation approach has been chosen, by testing two different sulfating agents, and the products are characterized from the molecular and physical-chemical point of view both in dilute and semi-dilute solutions. In addition, preliminary in vitro analyses are performed on mesenchymal stem cells to evaluate their biocompatibility and their ability to induce cell aggregation.

2. Materials and methods

Lactose-modified chitosan-hydrochloride form (CTL, previously reported as Chitlac) with fractions of *N*-acetyl-glucosamine (GlcNAc; “acetylated”, A) (FA) = 0.16; glucosamine ($GlcNH_2$; “deacetylated”, D) (FD) = 0.21; lactitol-substituted D unit (*N*-alkylated GlcNLac; “lactitol”, L) (FL) = 0.63 was kindly provided by BiopoLife S.r.L. (Trieste, Italy). An average repeating unit molecular weight equal to 400 g/mol was calculated for CTL on the basis of its composition. The intrinsic viscosity in 20 mM AcOH/AcONa at pH 4.5(Sacco et al., 2018) was 4.8 dL/g. Sodium chloride (NaCl), sodium hydroxide (NaOH), formamide, sulfur trioxide-pyridine complex, sulfur trioxide-*N*,*N*-dimethylformamide complex, deuterium oxide, ethylenediaminetetraacetic acid (EDTA), trisaminomethane (TRIS), phosphate-buffered-saline (PBS), in vitro Toxicology Assay Kit, Lactic Dehydrogenase based (TOX7) were purchased from Sigma Aldrich (USA). Penicillin/streptomycin, trypsin EDTA 1X, glutamine, fetal bovine serum (FBS) were purchased from Euroclone s.p.a. MesenPRO RS™ Medium from ThermoFisher Scientific (U.K.).

2.1. Sulfation reaction

A dry suspension of CTL (1.506 g, 3.765 mmol repeating unit) in formamide (30 mL) was stirred at 80 °C for 1 h to afford a colorless, viscous gel. After cooling to room temperature, the gel was treated with a suspension of sulfur trioxide-pyridine complex (SO_3·py, 4.158 g, 26.12 mmol) or sulfur trioxide-*N*,*N*-dimethylformamide (SO_3·DMF, 4.000 g, 26.12 mmol) in formamide (11 mL). After 24 h stirring at room temperature, a viscous solution was obtained. It was treated with a NaCl saturated solution in acetone (120 mL) to afford a white precipitate. After overnight storage at −28 °C, it was collected by carefully pouring the supernatant away and dried under vacuum to give a crude residue that was suspended in turn in pure water (30 mL) and then neutralized by adding some drops of a 33% w/v NaOH solution. After 3 h stirring at room temperature, the obtained yellowish, viscous solution was dialyzed and then freeze-dried to afford product **SC-1** (1.267 g, 84% mass yield; via sulfation with SO_3·py) or **SC-2** (1.818 g, 121% mass yield; via sulfation with SO_3·DMF) as a white fluffy solid.

2.2. NMR

NMR spectra were recorded on a Bruker Avance NEO (^{1}H: 600 MHz, ^{13}C: 150 MHz) or on a Bruker Avance III HD (^{1}H: 400 MHz, ^{13}C: 100 MHz) instrument (Billerica, MA, USA) – the former equipped with a cryo-probe – in D_2O (acetone as internal standard, ^{1}H: $(CH_3)_2CO$ at 2.22 ppm; ^{13}C:$(CH_3)_2CO$ at 31.5 ppm). Bruker TopSpin 4.0.5 software was used for all the experiments. Gradient-selected COSY and TOCSY experiments were performed using spectral widths of either 6000 Hz in both dimensions, using data sets of 2048 × 256 points. TOCSY mixing time was set to 120 ms. ^{1}H,^{13}C-DEPT-HSQC and ^{1}H,^{13}C-HSQC-TOCSY experiments were measured in the ^{1}H-detected mode via single quantum coherence with proton decoupling in the ^{13}C domain, using data sets of 2048 × 256 points and typically 100 increments.

2.3. Elemental analysis

C, H, N contents were determined in accordance with the ASTM D3176 protocol by using a Leco 628 elemental analyzer. Each measurements was repeated twice. Ethylenediaminetetraacetic acid (EDTA) was used as reference material for instrument calibration.

S content was measured in accordance with the ASTM D4239 protocol by using a Leco 144 analyzer. Each measurements was repeated twice. Vanadyl sulfate pentahydrate and a low sulfur coal (Leco 502-681) were used as reference materials for instrument calibration.

2.4. FT-IR

FT-IR spectra in the 4000–450 cm^{-1} range were recorded in transmission mode on a Perkin-Elmer MIR spectrophotometer. The spectra were acquired on pellets obtained upon the compression of powdered dispersions prepared by mixing and grinding each sample with KBr (~1 wt%). The spectra were acquired with a resolution of 1 cm^{-1} by collecting 8 scans and correcting the background noise.

2.5. Dynamic light scattering (DLS) analyses

DLS measurements were performed using a Zetasizer Nano ZS system (Malvern Istruments, Inc., Southborough, MA), to evaluate the intensity of 173° scattered light (Derived Count Rate – Kilocounts per second, kcps), the average hydrodynamic diameter, the polydisperity index (PDI) and the surface charge (ζ-potential) as a function of the pH of the solution and at pH 4.5 at different ionic strength. DLS measurements

were performed in triplicate at 25 °C. In all experiments, polymer concentration was 1 g/L.

2.6. Viscosity measurements

Intrinsic viscosity was measured at 25 °C by means of a Schott-Geräte AVS/G automatic measuring apparatus and an Ubbelohde-type capillary viscometer. Intrinsic viscosity [η] values were determined by analyzing the polymer concentration dependence of the reduced specific viscosity (η_{sp}/c) and of the reduced logarithm of the relative viscosity ($\ln(\eta_{rel})/c$) using the Huggins (Eq. (1)) and Kraemer (Eq. (2)) equations, respectively:

$$\frac{\eta_{sp}}{c} = [\eta] + k'[\eta]^2 c \quad (1)$$

$$\frac{ln(\eta_{rel})}{c} = [\eta] - k''[\eta]^2 c \quad (2)$$

where k′ and k″ are the Huggins and Kraemer constants, respectively. An aqueous Tris buffer (10 mM), pH 7.4 containing different concentrations of NaCl in the range 0.05 M–0.4 M was used as solvent.

2.7. Rheological measurements

Rheological tests were performed under continuous shear conditions to determine the steady viscosity values in the stress (τ) range 0.1–200 Pa, as well as under oscillatory shear conditions to determine the extension of the linear viscoelasticity regime (stress sweep tests at $\nu = 1$ Hz) and the mechanical spectrum (frequency sweep, $\tau = 1$ Pa, within the linear viscoelastic regime). The complex viscosity (η*), the storage (G′) and loss (G″) moduli were recorded in the frequency range 0.01–50 Hz. All tests were carried out with the controlled stress rheometer HAAKE MARS III operating typically at $T = 25$ °C. A glass bell covering the measuring device was used to improve thermal control and limit evaporation. A cone-plate CP60/1° geometry was used.

2.8. In vitro biocompatibility (LDH assay)

LDH assay (In vitro Toxicology Assay Kit, Lactic Dehydrogenase based, SIGMA) was employed to assess the biocompatibility of **SC-1** and **SC-2** on osteoblasts (Osteosarcoma MG-63 cell line). Cells were seeded at a density of 4×10^4 cells/well in 24-well plate and cultured in DMEM supplemented with 10% FBS and 0.25% penicillin/streptomycin, at 37 °C and 5% pCO_2. After 24 h the cells were treated with a solution of **SC-1** and **SC-2** 0.2% w/v in DMEM. Cells treated with Triton X-100 0.01% and cells cultured in plain medium were used as positive and negative control of cells death, respectively. The LDH assay was performed 24 and 72 h after treatment according to manufacturer's protocols. The percentage of LDH release was calculated by normalizing the absorbance values of each sample to the absorbance of the cellular lysis, at each time point considered. For each sample, four replicates were averaged.

2.9. Culture of hMSC-BM cells on polymer coated wells

In order to induce the formation of human Mesenchimal Bone Marrow Stem Cells (hMSC-BM) spheroids, the protocol explained by Donati et al. (2005), was employed. Briefly, 800 μL of a 2% w/V CTL-based solution were homogeneously distributed over the bottom of 12-well plate and allowed to air-drying overnight. Coated wells were sterilized under UV exposure. hMSC-BM at passage 3 were seeded at a density of 12×10^4 cells/well and maintained in culture for a 3 days at the most.

3. Results and discussion

3.1. Synthesis and characterization of sulfated lactose-modified chitosan samples

CTL is subjected to two different sulfation conditions that were mild enough to avoid per-*O*-sulfation and allow derivatization at the most reactive positions (i.e., amine and primary alcohol functionalities) (Bedini et al., 2017). Specifically, CTL is treated with formamide at 80 °C to obtain a highly viscous gel and then two different sulfating agents – sulfur trioxide complex with pyridine or *N*,*N*-dimethylformamide (SO_3·py or SO_3·DMF) – are added alternatively at room temperature (Scheme 1). After stirring overnight at room temperature, the sulfated derivatives **SC-1** and **SC-2** are obtained by precipitation followed by dialysis purification.

The presence of sulfur atoms in the two obtained polysaccharides is confirmed by elemental analysis, which reveals a degree of sulfation (DS) that is about twice as high for **SC-1** compared with **SC-2**. This result is unexpected due to known, higher reactivity for SO_3·DMF with respect to SO_3·py due to the lower Lewis base strength of DMF with respect to pyridine (Bedini et al., 2017). However, both **SC-1** and **SC-2** show a much lower DS value compared with the theoretical quantitative one (7.88, calculated as the number of sulfate groups per average repeating unit in the case of a per-*N*,*O*-sulfated product) (Table 1).

We confirm that the sulfur atoms are embedded in the polysaccharide backbone as sulfate monoesters from the FT-IR spectra of **SC-1** and **SC-2** (Fig. S1 in Supporting Information), which clearly show the presence of two intense bands at 1254 and 822 cm^{-1}, representing asymmetric S=O and symmetric C–O–S stretching vibrations, respectively, associated with a C–O–SO_3^- group (Fan et al., 2011) and which could not be detected in the spectrum of the parent compound CTL.

The ^{1}H NMR spectra of **SC-1** and **SC-2** (Fig. 1) confirm the presence of electron withdrawing functionalities – such as sulfate groups – that can cause a downfield shift of the hydrogen atom of a CH-OSO_3 moiety by about 0.5–0.8 ppm with respect to the parent CH-OH. To investigate the distribution of sulfate groups to the positions of the repeating polysaccharide units, 2D-NMR spectra for **SC-1** and **SC-2** are measured and analyzed. The DEPT-HSQC spectra of both reveal the presence of two groups of densities assigned by multiplicity tag to CH_2 atoms. The group of signals at $\delta_{H/C}$ 3.74–3.89/61.7–63.7 ppm could be attributed to CH_2OH units at position 6 of galactose (Gal) and glucitol (Glc-ol) units, as in the parent compound CTL (D'Amelio et al., 2013), while the ^{1}H and ^{13}C-downfield shifted methylene signals at $\delta_{H/C}$ 4.20–4.33/67.0–69.8 ppm could be assigned to their sulfated counterparts. Among the *CH* signals in the **SC-2** ^{1}H,^{13}C-DEPT-HSQC spectrum, three densities at significantly higher ^{1}H and ^{13}C-chemical shifts ($\delta_{H/C}$ 4.38/80.8, 4.47/78.7 and 4.74/77.6 ppm, respectively) are clearly identified with respect to CTL and therefore assigned to *CH* atoms bearing a sulfate monoester. Using other 2D-NMR spectra (COSY, TOCSY and HSQC-TOCSY), two of them could be assigned without doubt to 3-sulfated Gal *CH*-3 and 5-sulfated Glc-ol *CH*-5 atoms, while the most ^{1}H-downfield shifted one could not be assigned (Fig. 1). Downfield shifted signal related to 3-sulfated Gal *CH*-3 could also be detected in **SC-1** ^{1}H,^{13}C-DEPT-HSQC spectrum.

DS is estimated for each of the derivatized positions (Table 1), by relative integration of the signal volumes assigned to the same atoms in the sulfated and unsulfated case, respectively, assuming that they have similar $^1J_{C,H}$ coupling constants and that a deviation of about 5–8 Hz from the experimental set point does not cause a substantial variation in the integrated peak volumes (Vessella et al., 2021). It is worth noting that the backbone signals of CTL associated with amine and *N*-substituted glucosamine units (GlcN, GlcNAc, GlcNLac) are known to give very broad signals, which is due a shorter transverse relaxation time of the polysaccharide chain caused by a much lower overall tumbling (Donati et al., 2007). Thus, it is not possible to determine the presence of sulfate groups on the chitosan backbone of CTL by 2D-NMR analysis.

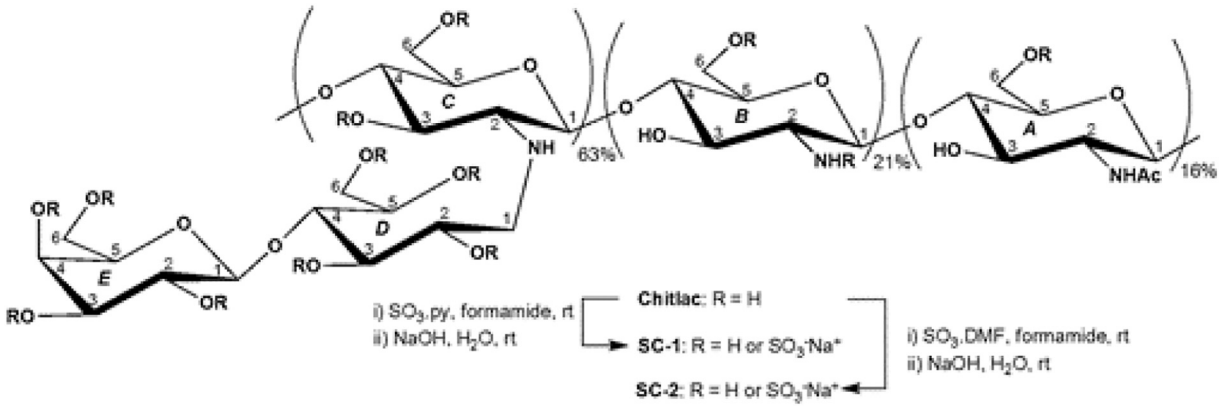

Scheme 1. Conversion of CTL into sulfated derivatives **SC-1** and **SC-2** (A = GlcNAc, B = GlcN, C = GlcNLac, D = Glc-ol, E = Gal).

Table 1
Yield and DS data for **SC-1** and **SC-2**.

	Yield[a] (%)	Total DS[b]	DS (lactitol-*O*-6)[c]	DS (Gal-*O*-3)[d]	DS (Glc-ol-*O*-5)[e]	DS (unknown)[f]
CTL	–	0.02 ± 0.01	–	–	–	–
SC-1	84%	2.75 ± 0.06	1.31	0.52	0.36	0.56 ± 0.06
SC-2	121%	1.32 ± 0.10	0.61	0.35	–	0.36 ± 0.10

[a] Mass yield calculated from starting CTL.
[b] Total DS calculated from elemental analysis data according to Eq. (1) (n_C = number of C atoms per average repeating unit = 13.88): DS = [(%S / atomic weight S) / (%C / atomic weight C)] * n_C (1).
[c] DS at Gal and Glc-ol *O*-6 site, as estimated by $^1H,^{13}C$-DEPT-HSQC spectra integration according to Eq. (2) (see also Fig. 2): DS (lactitol-*O*-6) = [I_{6S} / (I_{6S} + I_6)] * 2 (2).
[d] DS at Gal *O*-3 site, as estimated by $^1H,^{13}C$-DEPT-HSQC spectra integration according to Eq. (3) (see also Fig. 2): DS (Gal-*O*-3) = I_{3S} / (I_{3S} + I_3) (3).
[e] DS at Glc-ol *O*-5 site, as estimated by $^1H,^{13}C$-DEPT-HSQC spectra integration according to Eq. (4) (see also Fig. 2) DS (Glc-ol-*O*-5) = I_{5S} / (I_{5S} + I_5) (4)
[f] DS at not detected sites, as estimated by $^1H,^{13}C$-DEPT-HSQC spectra integration according to Eq. (5): DS (unknown) = Total DS – DS (lactitol-*O*-6) – DS (Gal-*O*-3) – DS (Glc-ol-*O*-5) (5).

Only the total DS related to unknown sulfated positions could be estimated, as the difference between the total DS obtained from elemental analysis and the sum of DS values at sulfated positions as evaluated by 2D-NMR (Table 1). Noteworthy, even if all the unassigned sulfated positions would be related to chitosan backbone of CTL, these represent only a minor amount (20–30%) of sulfate groups overall. The preference for sulfation of lactitol side-chains with respect to chitosan backbone is not surprising due to the reported higher flexibility of the former, that shows a good degree of solvation (at least in a simulated aqueous solvent; D'Amelio et al., 2013) and therefore a high propensity to react with sulfating agents present in solution.

3.2. Macromolecular properties of sulfated lactose-modified chitosan samples

Dynamic light scattering allows the aggregation of sulfated samples to be measured as a function of pH (Fig. 2a).

SC-2 shows a rather high scattering at a pH of about 2, which is higher than that of **SC-1**. This is due to the formation of aggregates between the chains caused by the electrostatic interactions between the negatively charged groups, i.e. the sulfates, and the positively charged amino groups in CTL. The two samples, i.e. **SC-1** and **SC-2**, differ in terms of the balance between negative and positive charges. Given the higher degree of sulfation, **SC-1** shows a greater imbalance between the oppositely charged groups and the positively charged ones, leading to limited aggregation, probably due to the repulsive contribution of the sulfate groups to each other. In contrast, a reduction in the negative charges on the polysaccharide backbone, as in **SC-2**, results in less repulsion between the chains and thus higher aggregation. However, in both cases of **SC-1** and **SC-2**, increasing the pH leads to a decrease in aggregation. This is due to the very low residual charge of the amino groups of the glucosamine units at a pH of about 7. Therefore, the sulfated samples behave like polyanions and the electrostatic repulsion hinders aggregation.

The ζ-potential for the two sulfated samples gives a similar picture (Fig. 2b). A low pH leads to aggregation with an excess of negative charge and a more negative ζ-potential. However, when the pH increases, the ζ-potential increases and reaches the value that is essentially determined by the amount of sulfated groups on the polysaccharide chains. In this sense, the ζ-potential shows a higher amount of sulfated groups and consequently a lower value of ζ-potential, for **SC-1** compared to **SC-2**, in agreement with the NMR analyses.

An additional DLS analysis is performed on the scattering of **SC-1** and **SC-2** as a function of the ionic strength of the aqueous solution (Fig. 3) at pH 4.5.

In the absence of added salt (high Debye length), only limited formation of complexes occurs due to repulsion between chains, which prevents aggregation. However, increasing the ionic strength up to a NaCl concentration of 0.15 M leads to aggregation due to the shielding the repulsion between the negative charges which is more pronounced for **SC-1**. This could be due to both the higher molecular weight and the degree of sulfation. A similar result was also observed with mixtures of CTL with polyanions such as alginate (Donati et al., 2007). Further increasing in the ionic strength, i.e. in the presence of 0.3 M aqueous NaCl, prevents strong aggregation of the sulfated samples by shielding the electrostatically attractive interaction.

The effect of ionic strength on the intrinsic viscosity of the samples was observed at pH 7.4 (Fig. 4).

Experimental data show that both CTL and **SC-2** have a low dependence on ionic strength, which differs from **SC-1**. These results were evaluated using the Smidsrød B parameter (Eq. (3)):

$$B = \frac{S}{\left([\eta]_{0.1}\right)^{1.3}} \tag{3}$$

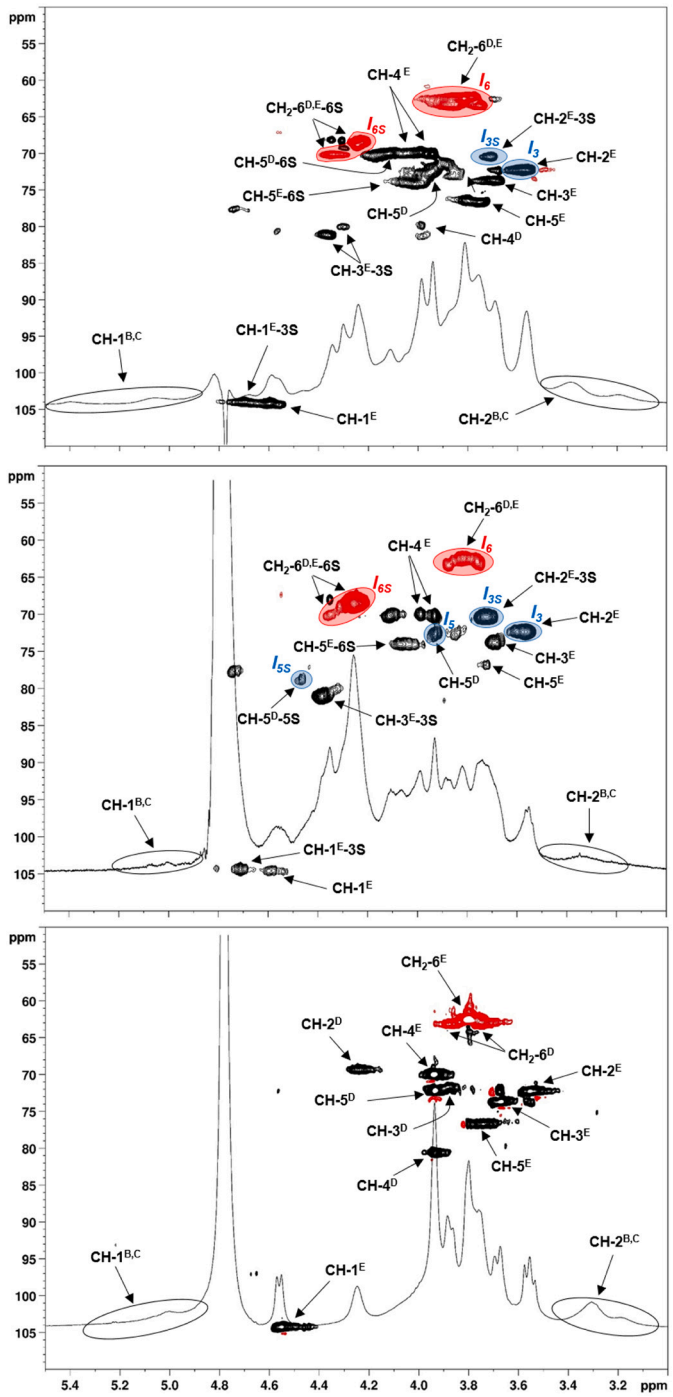

Fig. 1. ^{1}H and ^{1}H,^{13}C-DEPT-HSQC NMR spectra (600 MHz, 298 K, D_2O, zoom) of CTL (bottom), **SC-1** (middle) and **SC-2** (top) (densities enclosed in the highlighted areas were integrated for the estimation of relative amounts of differently sulfated units: see Table 1 for details; see Scheme 1 for CTL residues numbering).

where S is the slope of the dependence of the intrinsic viscosity on $I^{-1/2}$and $[\eta]_{0.1}$is the intrinsic viscosity measured in the presence of NaCl 0.1 M. The higher is the Smidsrød B parameter, the more flexible is the charged polysaccharide backbone (typically B ranges from $5.25{\cdot}10^{-3}$ for a very rigid molecule such as xanthan (Tinland & Rinaudo, 1989) to 0.2 for carboxymethylamylose (Smidsrød & Haug, 1971)). The evaluation of the Smidsrød's B parameter is an effective way to express the rigidity of the polysaccharide for both polyanions and polycations (Anthonsen et al., 1993a).

Intrinsic viscosity does not vary with the ionic strength for a neutral (or nearly neutral) polysaccharide. The data obtained for the original and sulfated CTL samples are shown in Table 2.

Unmodified CTL shows a very low dependence of intrinsic viscosity on ionic strength due to the limited residual positive charge at pH 7.4 (zeta-potential + 6.8 mV) (Donati et al., 2007). This is reflected in a Smidsrød's B parameter of $5{\cdot}10^{-3}$. When sulfate groups are introduced into CTL backbone, the overall charge is determined by the balancing of the positive and negative charges. Introducing a limited amount of sulfate groups, as in **SC-2**, results in an overall slightly negative charge, as shown in Fig. 4b, with a low Smidsrød's B parameter of about $5.5{\cdot}10^{-2}$. In contrast, when the amount of sulfate groups is increased, as in **SC-1**, the Smidsrød's B parameter increases to 0.1, which, compared to literature values for various polyelectrolytes, describes the sulfated polymer as flexible.

The analysis of Fig. 5 allows determining the intrinsic viscosity at infinite ionic strength, $[\eta]_{\infty}$, as (Eq. (4)):

$$[\eta]_I = [\eta]_{\infty} + SI^{-1/2} \tag{4}$$

The results are shown in Table 2. It is confirmed that the chemical procedure used to modify CTL results in a significant reduction in the molecular weight of the polysaccharide. Of the two sulfated samples, i.e., **SC-1** and **SC-2**, the latter exhibits a more compact structure which, in turn, could be due to higher degradation by the synthetic conditions used.

Based on the intrinsic viscosity at infinite ionic strength, the molecular weight of the sulfated sample is determined assuming an unperturbed random coil (Eq. (5)) (Table 3):

$$[\eta]_{I=\infty} = \Phi \frac{\left(\overline{h^2}_0\right)^{\frac{3}{2}}}{M} = \Phi M^{0.5} \tag{5}$$

where Φ is a parameter which is a function of the spatial distribution of the chain molecule units.

It has already been shown that the absence of rigid kinks represented by acetyl groups along the chain allows the use of the unperturbed random coil statistics for chitosan at infinite ionic strength (Anthonsen et al., 1993b). This is also true for CTL at neutral pH, given the known flexibility of the chain as determined by Smidsrød's B value in this work and by molecular dynamics calculations (Esteban et al., 2018) and the low residual charge of the polysaccharide. Although the value Φ is not constant, in chitosan samples it appears to be influenced by the intrinsic flexibility of the polymer chain rather than by electrostatic repulsion between charged groups (Anthonsen et al., 1993b).

The molecular weight of the two sulfated samples is determined using the same Φ calculated for CTL, since the polysaccharide contains relatively few negative charges. The results show that the conditions required for the synthesis of **SC-1** result in a net decrease in the molecular weight. However, for **SC-2**, even harsher conditions are required and the chain cleavage is even more dramatic.

The reduction of the total ionic strength could cause an expansion of the whole polysaccharide compared to the unperturbed dimension, which is caused by the expansion factor, α (Eq. (6)):

$$\overline{h^2} = \alpha^2 \overline{h^2}_0 \tag{6}$$

Considering the condition of NaCl 0.1 M, Eq. (5) becomes Eq. (7):

$$[\eta]_{0.1M} = \Phi \frac{\left(\overline{h^2}\right)^{\frac{3}{2}}}{M} \tag{7}$$

Thus, in the perturbed dimension, the following relationship holds between intrinsic viscosity and molecular weight (Eq. (8)):

$$[\eta]_{0.1M} = KM^{a} \tag{8}$$

Assuming that all samples have the same K, the values a were calculated (Table 3). CTL shows basically no variation in term of

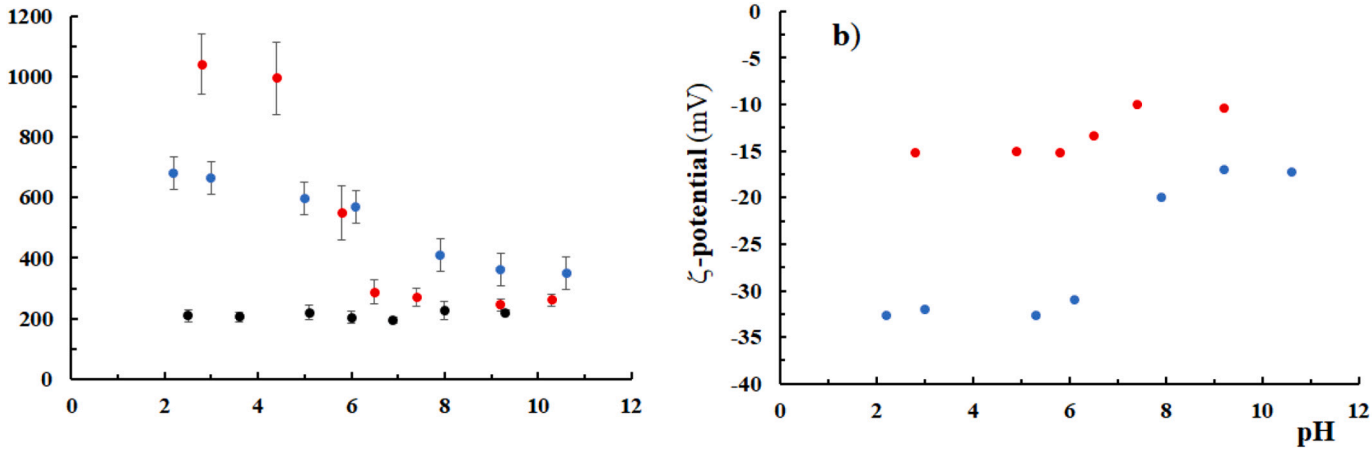

Fig. 2. **a**) Intensity of the scattered light and **b**) ζ-potential as a function of the pH for CTL (black), **SC-1** (blue) and **SC-2** (red), respectively. Polymer concentration: 1 g/L.

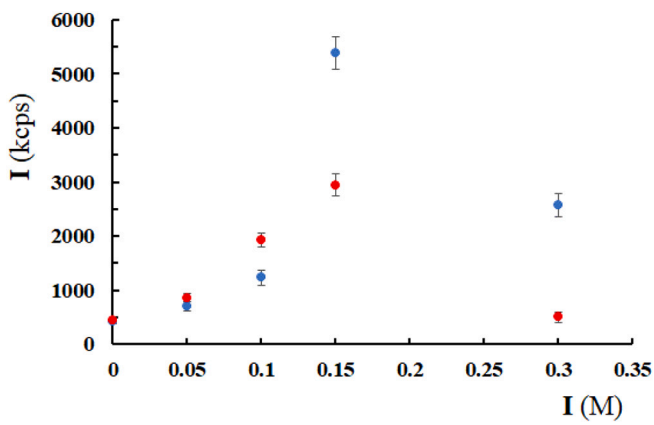

Fig. 3. Dependence of the intensity of the scattered light on the ionic strength of the added sodium chloride in the aqueous solution for **SC-1** (blue) and **SC-2** (red), respectively. Conditions: polymer concentration = 1 g/L, buffer: AcOH/AcONa 20 mM, pH 4.5.

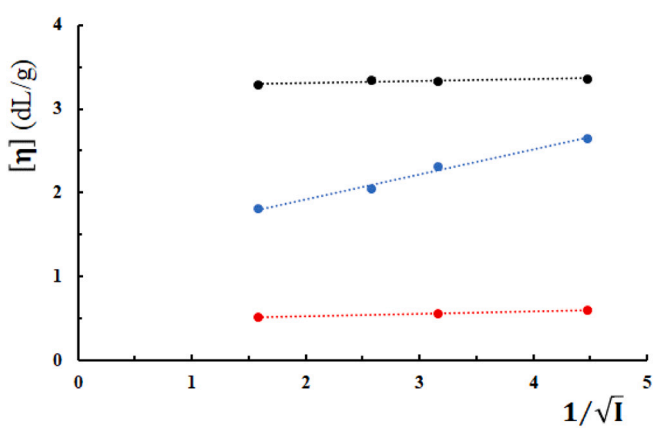

Fig. 4. Dependence of the intrinsic viscosity on the inverse of the square root of the ionic strength for CTL (black), **SC-1** (blue) and **SC-2** (red), respectively. Buffer: Tris 20 mM, pH 7.4.

Table 2
Intrinsic viscosity at 0.1 M NaCl and at infinite ionic strength, S and B for the three samples considered in the present study.

Sample	$[\eta]_{0.1}$ (dL/g)[a]	$[\eta]_{\infty}$ (dL/g)[b]	S	B
CTL	3.33	3.25	0.024	0.005
SC-1	2.31	1.33	0.297	0.1
SC-2	0.56	0.48	0.026	0.055

molecular weight dependence of the intrinsic viscosity. It can therefore be described as unperturbed even in the presence of NaCl 0.1 M, most likely due to the very low residual positive charge and flexibility. The presence of a small amount of sulfate groups on the polymer chain in **SC-2**, as determined by the slightly negative zeta-potential (Fig. 2b), leads to a limited expansion of the polysaccharide chain and to a parameter slightly higher than 0.5, i.e. 0.515. This means that the coils are slightly expanded in NaCl 0.1 M, which is then a slightly good solvent. An even more pronounced effect is observed for **SC-1**. In this case, the solvent NaCl 0.1 M becomes a good solvent, and the prameter a was calculated to be 0.545.

The unmodified and sulfated CTL samples were analyzed under semi-dilute conditions, and the flow curves and mechanical spectra were recorded (Fig. 5).

The mechanical spectra show that the polysaccharide as such and sulfated ones behave like solutions in all cases, with G″ being higher than G′. In addition, degradation by the synthetic protocol is evident from the lower viscous response.

The experimental flow curves were modeled using the Cross equation (Sacco et al., 2017) and the zero-shear viscosity, $\eta_{\dot{\gamma}\to 0}$, was calculated (Table 3) showing the clear effect of the reduction in molecular weight due to the chemical modification.

It has already been reported (Morris et al., 1981) that for concentrated solutions where c[η] is greater than 4, the following scaling law holds (Eq. (9)):

$$\eta \propto M^{3.3} \tag{9}$$

The concentrated solution condition is met by CTL and **SC-1**, and for the latter, an attempt was made to determine the molecular weight based on the value known for the former polysaccharide (Table 3). Although the molecular weight determined on the basis of Eq. (9) for the sulfated sample is, in a strict sense, significantly higher than that

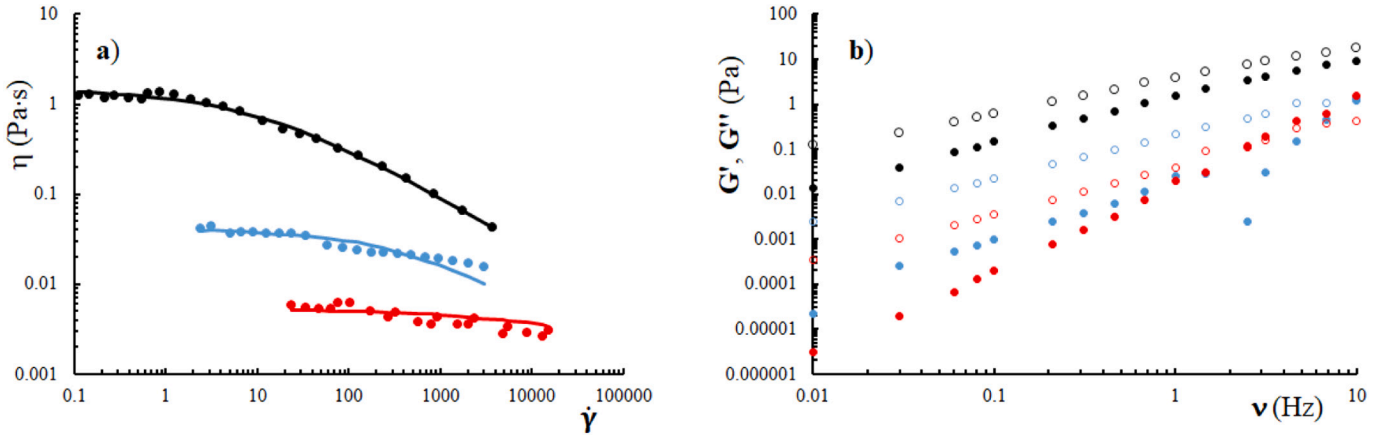

Fig. 5. a) Dependence of the shear viscosity on the shear rate for CTL (black dots), SC-1 (blue dots) and SC-2 (red dots), respectively. Continuous line represents the best fit of the experimental data with the Cross equation. b) Dependence of the storage (G′, full dots) and loss (G″, open dots) moduli from frequency for CTL (black), SC-1 (blue) and SC-2 (red), respectively. Buffer: Tris 20 mM, pH 7.4.

Table 3
Estimated molar mass, a parameter and zero-shear viscosity for the three samples considered in the present study.

Sample	Mw	a[a]	$\eta_{\dot{\gamma}\to 0}$[b] (mPa·s)	Mw[c]
CTL	800,000	0.502	1452	800,000
SC-1	130,000	0.547	41	270000[d] 190000[e]
SC-2	17,000	0.515	5.6	

[a] Calculated starting from the molecular weight of the first column.
[b] Calculated from the application of the Cross equation to the flow curves reported in Fig. 6a.
[c] Calculated form the zero-shear viscosity of semi-dilute solutions using Eq. (9) with power [d] 3.3 or [e] 3.4.

determined on the basis of intrinsic viscosity, it should be emphasized that a slight increase in the power law to 3.4 does bring the two determinations in agreement.

3.3. Biological properties

The biocompatibility of the sulfated samples along with that of the unmodified CTL is preliminary evaluated using the MG-63 cell line and no significant differences in terms of LDH release from the cytoplasm of cells is observed between the samples (data not shown).

The three samples are compared in terms of their ability to induce aggregation of mesenchymal stem cells and the results are reported in Fig. 6.

Previous studies have shown that CTL induces aggregation of primary chondrocytes with the formation of high-dimensional nodules within 12–24 h (Donati et al., 2005). Recently, cell aggregation promoted by lactose derivatives of chitosan was found to be a prerequisite for the commitment of adipose-derived stem cells to the chondrogenic lineage (Tan et al., 2013). Here, we showed that both **SC-1** and **SC-2** induced the formation of aggregates after one day of culture (Fig. 6a), showing evident differences from those with CTL. The number of spheroids formed by the sulfated samples is higher (Fig. 6b), but their area is much smaller (Fig. 6c). Interestingly, at day 1 there are also differences in the area of spheroids formed by the sulfated polymers. In particular, **SC-2** induces the formation of spheroids smaller than those obtained from **SC-1**. Moreover, in the samples with **SC-2**, the presence of isolated cells can still be observed. These cells are not involved in the formation of aggregates and they manage to adhere and spread regardless of the presence of the polymer. Over time, the differences between the three samples become even more evident. The spheroids with CTL and **SC-1** increase their size for a clear effect of physical aggregation between them albeit the phenomenon is more pronounced in the case of CTL. In the case of **SC-2**, it is no longer possible to observe spheroids in suspension on day 3, but the few still present have settled on the surface. Many cells spread and a cellular network has formed on the surface of the plastic. Overall, both **SC-1** and **SC-2** act differently in cell aggregation. **SC-1** has a higher degree of sulfation and lower degradation, and these properties are fundamental for the formation of spheroids similar to CTL. On the other hand, the high degradation of **SC-2** invalidates the aggregation process, leading to adhesion of spheroids to the surface and spreading of single cells. Spheroids derived from mesenchymal stem cells are considered as a basis for scaffold-free tissue engineering and 3D cartilage differentiation models (Kronemberger et al., 2020). One of the limitations associated with the use of cell systems in the form of spheroids both in vitro and in vivo is represented by the difficulty of gaseous and nutritional exchanges between the nucleus of the spheroid and the outside. This phenomenon will appear more evident the larger is the diameter of the structure. This often results in the formation of necrotic areas within the spheroid. This has been observed when CTL is used for cell aggregation. From this point of view, the small dimensions maintained by spheroids formed in presence of **SC-1** certainly lead to advantages in terms of viability and nutrient exchange during the period useful for cartilage differentiation of mesenchymal stem cells.

4. Conclusions

Sulfate glycosaminoglycans are one of the major components of native cartilage and play an important role in the signal transduction and phenotype of resident chondrocytes. The approach described in this article leads to the synthesis of two sulfated lactose-modified chitosan derivatives (**SC-1** and **SC-2**) with different degrees of sulfation (DS). It has been shown that most of the sulfation mainly affects the flexible side chains of the polysaccharide and the contemporary presence of negative and positive charges leads to chain-chain aggregation which is influenced by the presence of supporting salt. The negative charge inserted is accompanied by a high flexibility of the polysaccharide chain. However, the synthetic approach leads to a marked chain cleavage which has to be taken into consideration for potential applications of these derivatives. Indeed, further work will be focused on incrementing the sulfation degree while limiting the decrease of the molecular mass.

The products obtained are biocompatible thus allowing their use in contact with different cell lines. A very promising aspect is the fact that they induce the aggregation of mesenchymal stem cells. It is likely that this ability is also maintained when primary chondrocytes are used thus showing a very good potential for the applications in the field of

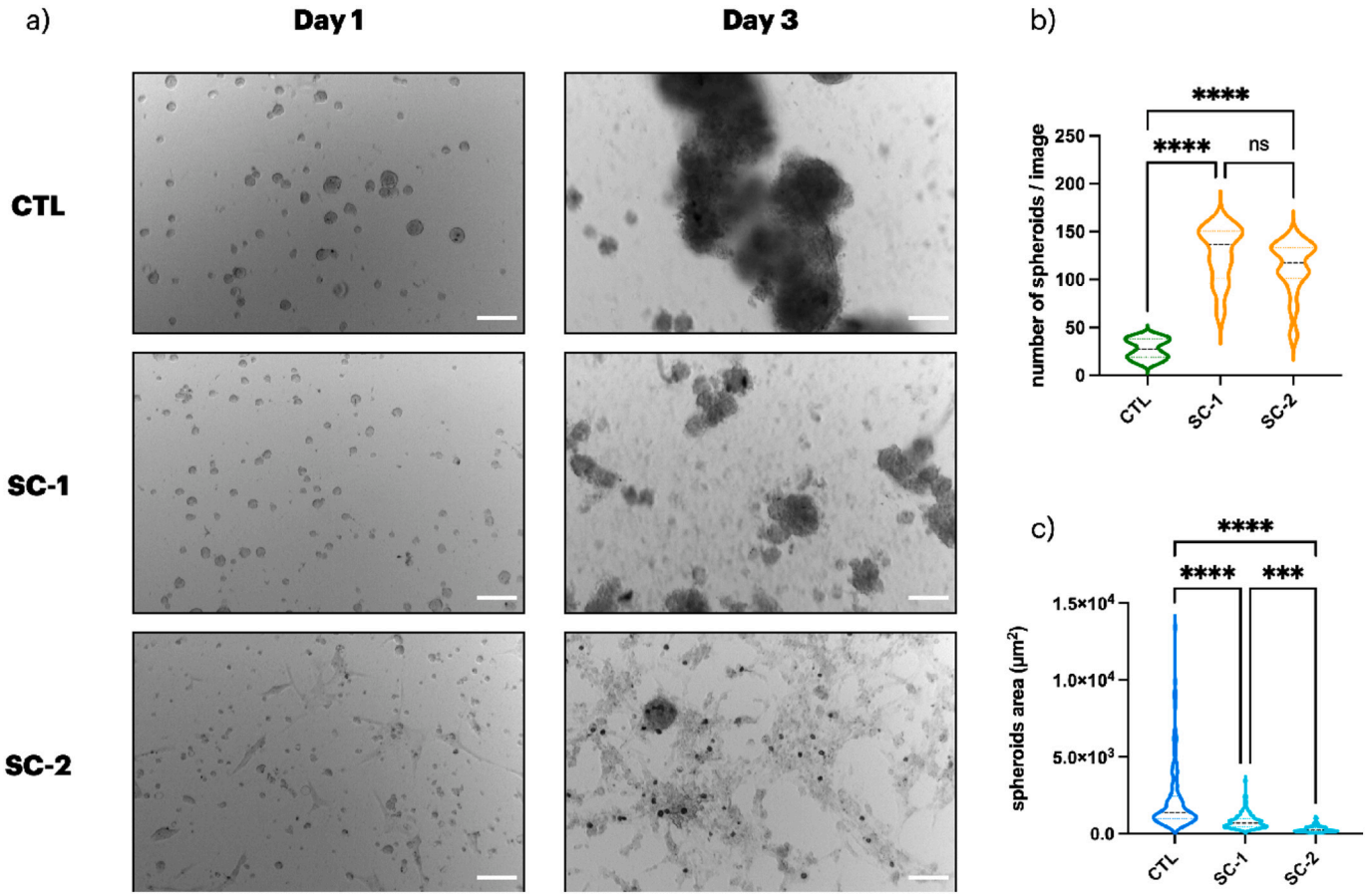

Fig. 6. Optical Images of hMSC-BM spheroids at different investigated time points. Scale bars are 150 µm (a). Number of spheroids per image (b) and spheroids area (c) after 1 day of incubation in cell culture medium. Data are reported as violin plots showing the median of values ($n = 13–15$ images analyzed in b and $n = 145–150$ spheroids analyzed in c). Statistics: ns, not significant; ****, $p < 0.0001$; One way Anova followed by Tukey's multiple comparisons test.

cartilage regenereation. Chondroitin sulfate has attracted great attention as a biomaterial for cartilage tissue engineering (Shin et al., 2021) and the idea of using mesenchymal stem cells in combination with this polymer is already being used as an in vitro model for the study of osteoarthritis (Pérez-Castrillo et al., 2021). It follows that the possibility of combining 3D cell systems with biomimetic semi-synthetic sulfated polymers mimicking GAGs chemistry could represent an advantageous strategy.

However, a more in-depth study on the viability, differentiation, and production of GAG mimics is needed to gain more information on the use of sulfated lactose-modified chitosan in biomaterial development.

Supplementary data to this article can be found online at https://doi.org/10.1016/j.carbpol.2022.119379.

CRediT authorship contribution statement

Chiara Pizzolitto: Investigation, Writing – original draft. **Fabiana Esposito:** Investigation, Writing – original draft. **Pasquale Sacco:** Investigation, Writing – original draft. **Eleonora Marsich:** Conceptualization, Writing – review & editing. **Valentina Gargiulo:** Conceptualization, Writing – review & editing. **Emiliano Bedini:** Conceptualization, Writing – review & editing. **Ivan Donati:** Conceptualization, Writing – review & editing.

Declaration of competing interest

The authors declare that they have no known competing financial interests or personal relationships that could have appeared to influence the work reported in this paper.

References

Aisenbrey, E. A., & Murphy, W. L. (2020). Synthetic alternatives to Matrigel. *Nature Reviews Materials, 5*(7), 539–551.

Anthonsen, M. W., Vårum, K. M., & Smidsrød, O. (1993a). Solution properties of chitosans: Conformation and chain stiffness of chitosans with different degrees of N-acetylation. *Carbohydrate Polymers, 22*(3), 193–201.

Anthonsen, M. W., Vårum, K. M., & Smidsrød, O. (1993b). Solution properties of chitosans: Conformation and chain stiffness of chitosans with different degrees of N-acetylation. *Carbohydrate Polymers, 22*(3), 193–201.

Bedini, E., Laezza, A., Parrilli, M., & Iadonisi, A. (2017). A review of chemical methods for the selective sulfation and desulfation of polysaccharides. *Carbohydrate Polymers, 174*, 1224–1239.

Bedini, E., Corsaro, M. M., Fernández-Mayoralas, A., & Iadonisi, A. (2019). In E. Cohen, & H. Merzendorfer (Eds.), *Chondroitin, dermatan, heparan, and keratan sulfate: Structure and functions BT - Extracellular sugar-based biopolymers matrices* (pp. 187–233). Springer International Publishing.

Berven, L., Solberg, R., Truong, H., Arlov, Ø., Aachmann, F., Skjåk-Bræk, G., Jacobsen, W., Johansen, H., & Samuelsen, A. (2013). Alginates induce legumain activity in RAW 264.7 cells and accelerate autoactivation of prolegumain. *Bioactive Carbohydrates and Dietary Fibre, 2*, 30–44.

Bishnoi, M., Jain, A., Hurkat, P., & Jain, S. K. (2016). Chondroitin sulphate: A focus on osteoarthritis. *Glycoconjugate Journal, 33*(5), 693–705.

Cesarz, Z., & Tamama, K. (2016). Spheroid culture of mesenchymal stem cells. *Stem Cells International, 2016*, 9176357.

D'Amelio, N., Esteban, C., Coslovi, A., Feruglio, L., Uggeri, F., Villegas, M., Benegas, J., Paoletti, S., & Donati, I. (2013). Insight into the molecular properties of chitlac, a chitosan derivative for tissue engineering. *The Journal of Physical Chemistry B, 117*(43), 13578–13587.

Donati, I., Stredanska, S., Silvestrini, G., Vetere, A., Marcon, P., Marsich, E., Mozetic, P., Gamini, A., Paoletti, S., & Vittur, F. (2005). The aggregation of pig articular chondrocyte and synthesis of extracellular matrix by a lactose-modified chitosan. *Biomaterials, 26*(9), 987–998.

Donati, I., Borgogna, M., Turello, E., Casàro, A., & Paoletti, S. (2007). Tuning supramolecular structuring at the nanoscale level: Nonstoichiometric soluble complexes in dilute mixed solutions of alginate and lactose-modified chitosan (Chitlac). *Biomacromolecules, 8*(5), 1471–1479.

Doncel-Pérez, E., Aranaz, I., Bastida, A., Revuelta, J., Camacho, C., Acosta, N., Garrido, L., Civera, C., García-Junceda, E., Heras, A., & Fernández-Mayoralas, A. (2018). Synthesis, physicochemical characterization and biological evaluation of chitosan sulfate as heparan sulfate mimics. *Carbohydrate Polymers, 191*, 225–233.

Esteban, C., Donati, I., Pantano, S., Villegas, M., Benegas, J., & Paoletti, S. (2018). Dissecting the conformational determinants of chitosan and chitlac oligomers. *Biopolymers, 109*(6), Article e23221.

Fan, L., Jiang, L., Xu, Y., Zhou, Y., Shen, Y., Xie, W., Long, Z., & Zhou, J. (2011). Synthesis and anticoagulant activity of sodium alginate sulfates. *Carbohydrate Polymers, 83*(4), 1797–1803.

Guerrini, M., Beccati, D., Shriver, Z., Naggi, A., Viswanathan, K., Bisio, A., Capila, I., Lansing, J. C., Guglieri, S., Fraser, B., Al-Hakim, A., Gunay, N. S., Zhang, Z., Robinson, L., Buhse, L., Nasr, M., Woodcock, J., Langer, R., Venkataraman, G. Sasisekharan, R., … (2008). Oversulfated chondroitin sulfate is a contaminant in heparin associated with adverse clinical events. *Nature Biotechnology, 26*(6), 669–675.

Kronemberger, G. S., Matsui, R. A. M., Miranda, G. A. S. C. E., Granjeiro, J. M., & Baptista, L. S. (2020). Cartilage and bone tissue engineering using adipose stromal/stem cells spheroids as building blocks. *World Journal of Stem Cells, 12*(2), 110–122.

Marcon, P., Marsich, E., Vetere, A., Mozetic, P., Campa, C., Donati, I., Vittur, F., Gamini, A., & Paoletti, S. (2005). The role of Galectin-1 in the interaction between chondrocytes and a lactose-modified chitosan. *Biomaterials, 26*(24), 4975–4984.

Marsich, E., Borgogna, M., Donati, I., Mozetic, P., Strand, B. L., Salvador, S. G., Vittur, F., & Paoletti, S. (2008). Alginate/lactose-modified chitosan hydrogels: A bioactive biomaterial for chondrocyte encapsulation. *Journal of Biomedical Materials Research - Part A, 84*(2), 364–376.

Medelin, M., Porrelli, D., Aurand, E. R., Scaini, D., Travan, A., Borgogna, M. A., Cok, M., Donati, I., Marsich, E., Scopa, C., Scardigli, R., Paoletti, S., & Ballerini, L. (2018). Exploiting natural polysaccharides to enhance in vitro bio-constructs of primary neurons and progenitor cells. *Acta Biomaterialia, 73*, 285–301.

Morris, E. R., Cutler, A. N., Ross-Murphy, S. B., Rees, D. A., & Price, J. (1981). Concentration and shear rate dependence of viscosity in random coil polysaccharide solutions. *Carbohydrate Polymers, 1*(1), 5–21.

Pérez-Castrillo, S., González-Fernández, M. L., Álvarez-Suárez, J., Sánchez-Lázaro, J., Esteban-Blanco, M., Gutiérrez-Velasco, L., González-Cubero, E., & Villar-Suárez, V. (2021). Effect of mesenchymal stem cells combined with chondroitin sulfate in an in vitro model of osteoarthritis. *American Journal of Translational Research, 13*(6), 5928–5942.

Pizzolitto, C., Cok, M., Asaro, F., Scognamiglio, F., Marsich, E., Lopez, F., Donati, I., & Sacco, P. (2020). On the mechanism of genipin binding to primary amines in lactose-modified chitosan at neutral pH. *International Journal of Molecular Sciences, 21*(18), 6831.

Reginster, J.-Y., Dudler, J., Blicharski, T., & Pavelka, K. (2017). Pharmaceutical-grade chondroitin sulfate is as effective as celecoxib and superior to placebo in symptomatic knee osteoarthritis: The ChONdroitin versus CElecoxib versus Placebo trial (CONCEPT). *Annals of the Rheumatic Diseases, 76*(9), 1537–1543.

Revuelta, J., Aranaz, I., Acosta, N., Civera, C., Bastida, A., Peña, N., Monterrey, D. T., Doncel-Pérez, E., Garrido, L., Heras, Á., García-Junceda, E., & Fernández-Mayoralas, A. (2020). Unraveling the structural landscape of chitosan-based heparan sulfate mimics binding to growth factors: Deciphering structural determinants for optimal activity. *ACS Applied Materials & Interfaces, 12*(23), 25534–25545.

Sacco, P., Furlani, F., Cok, M., Travan, A., Borgogna, M., Marsich, E., Paoletti, S., & Donati, I. (2017). Boric acid induced transient cross-links in lactose-modified chitosan (Chitlac). *Biomacromolecules, 18*(12), 4206–4213.

Sacco, P., Cok, M., Asaro, F., Paoletti, S., & Donati, I. (2018). The role played by the molecular weight and acetylation degree in modulating the stiffness and elasticity of chitosan gels. *Carbohydrate Polymers, 196*, 405–413.

Sacco, P., Cok, M., Scognamiglio, F., Pizzolitto, C., Vecchies, F., Marfoglia, A., Marsich, E., & Donati, I. (2020). Glycosylated-chitosan derivatives: A systematic review. *Molecules, 25*(7), 1534.

Sart, S., Tsai, A.-C., Li, Y., & Ma, T. (2014). Three-dimensional aggregates of mesenchymal stem cells: Cellular mechanisms, biological properties, and applications. *Tissue Engineering. Part B, Reviews, 20*(5), 365–380.

Schneider, H., Maheu, E., & Cucherat, M. (2012). Symptom-modifying effect of chondroitin sulfate in knee osteoarthritis: A meta-analysis of randomized placebo-controlled trials performed with structum(®). *The Open Rheumatology Journal, 6*, 183–189.

Shin, J., Kang, E. H., Choi, S., Jeon, E. J., Cho, J. H., Kang, D., Lee, H., Yun, I. S., & Cho, S.-W. (2021). Tissue-adhesive chondroitin sulfate hydrogel for cartilage reconstruction. *ACS Biomaterials Science & Engineering, 7*(9), 4230–4243.

Shute, J. (2012). In R. Lever, B. Mulloy, & C. P. Page (Eds.), *Glycosaminoglycan and chemokine/growth factor interactions BT-heparin - A century of progress* (pp. 307–324). Berlin Heidelberg: Springer.

Silbert, J. E., & Sugumaran, G. (2002). Biosynthesis of chondroitin/dermatan sulfate. *IUBMB Life, 54*(4), 177–186.

Smidsrød, O., & Haug, A. (1971). Estimation of the relative stiffness of the molecular chain in polyelectrolytes from measurements of viscosity at different ionic strengths. *Biopolymers, 10*(7), 1213–1227.

Tan, H., Lao, L., Wu, J., Gong, Y., & Gao, C. (2008). Biomimetic modification of chitosan with covalently grafted lactose and blended heparin for improvement of in vitro cellular interaction. *Polymers for Advanced Technologies, 19*(1), 15–23.

Tan, H., Wu, J., Huang, D., & Gao, C. (2010). The design of biodegradable microcarriers for induced cell aggregation. *Macromolecular Bioscience, 10*(2), 156–163.

Tan, H., Gao, X., Sun, J., Xiao, C., & Hu, X. (2013). Double stimulus-induced stem cell aggregation during differentiation on a biopolymer hydrogel substrate. *Chemical Communications, 49*(98), 11554–11556.

Tarricone, E., Mattiuzzo, E., Belluzzi, E., Elia, R., Benetti, A., Venerando, R., Vindigni, V., Ruggieri, P., & Brun, P. (2020). Anti-inflammatory performance of lactose-modified chitosan and hyaluronic acid mixtures in an in vitro macrophage-mediated inflammation osteoarthritis model. *Cells, 9*(6), 1328.

Tinland, B., & Rinaudo, M. (1989). Dependence of the stiffness of the xanthan chain on the external salt concentration. *Macromolecules, 22*(4), 1863–1865.

Travan, A., Marsich, E., Donati, I., Foulc, M.-P., Moritz, N., Aro, H. T., & Paoletti, S. (2012). Polysaccharide-coated thermosets for orthopedic applications: From material characterization to in vivo tests. *Biomacromolecules, 13*(5), 1564–1572.

Vessella, G., Traboni, S., Cimini, D., Iadonisi, A., Schiraldi, C., & Bedini, E. (2019). Development of semisynthetic, regioselective pathways for accessing the missing sulfation patterns of chondroitin sulfate. *Biomacromolecules, 20*(8), 3021–3030.

Vessella, G., Esposito, F., Traboni, S., Di Meo, C., Iadonisi, A., Schiraldi, C., & Bedini, E. (2021). Exploiting diol reactivity for the access to unprecedented low molecular weight curdlan sulfate polysaccharides. *Carbohydrate Polymers, 269*, Article 118324.